

# Lawrence Berkeley National Laboratory

## Lawrence Berkeley National Laboratory

### **Title**

Mathematical Models of Feedback Systems for control of Intra-bunch Instabilities Driven by EClouds and TMCI

### **Permalink**

<https://escholarship.org/uc/item/07r6c1wz>

### **Author**

Rivetta, C.H.

### **Publication Date**

2012-05-01

# MATHEMATICAL MODELS OF FEEDBACK SYSTEMS FOR CONTROL OF INTRA-BUNCH INSTABILITIES DRIVEN BY E-CLOUDS AND TMCI \*

C. Rivetta <sup>†</sup>, J.D. Fox, T. Mastorides, M. Pivi, O. Turgut, SLAC, Stanford, USA,  
W. Hofle, CERN, Geneva, Switzerland, and R. Secondo, J.-L. Vay, LBNL, Berkeley, USA

## Abstract

The feedback control of intra-bunch instabilities driven by electron-clouds or strong head-tail coupling (transverse mode coupled instabilities TMCI) requires bandwidth sufficient to sense the vertical position and apply correction fields to multiple sections of a nanosecond-scale bunch. These requirements impose challenges and limits in the design and implementation of the feedback control channel.

This paper presents different models for the feedback subsystems: receiver, processing channel, amplifier and kicker, that take into account their frequency response and limits. These models are included in reduced mathematical models of the bunch dynamics and multi-particle simulation codes (WARP / C-MAD / HEADTAIL) to evaluate the impact of the subsystem limitations in the bunch stabilization and emittance improvement. With this realistic model of the hardware, it is possible to analyze and design the feedback system. This research is crucial to evaluate the boundary in the performance of the feedback control system due to technological limitations. Additionally, these models define the impact of parameter variations or mismatching and the effect of spurious perturbation and noise in the performance of the feedback system.

## INTRODUCTION

Intra-bunch instabilities induced by electron clouds and strong head-tail interactions are one of the limiting factors to reach the maximum beam currents in the SPS ring [1]. Feedback techniques can stabilize bunch instabilities induced not only by e-clouds but also by strong head-tail interactions (TMCI). DOE US LHC Accelerator Research Program (LARP) is supporting a collaboration between US Labs and CERN to study the viability of controlling intra-bunch instabilities using feedback control techniques. A collaboration among SLAC / LBNL / CERN started evaluating the limitations of this technique to mitigate both instabilities and other possible head-tail distortions in bunches [2] [3].

The application of feedback control to stabilize the bunch is challenging because it requires sufficient bandwidth to sense the transverse position and apply correcting fields to different parts of a nanosecond-scale bunch. These requirements impose technology challenges and limits in the design [4]. Additionally, from a feedback stand-point the intra-bunch dynamics is more challenging to model and

control than the beam dynamics involving the interaction between bunches. Given the machine schedule limitations to test and install a prototype feedback system in the SPS ring, non-linear simulators based on multi-particle description of the bunch and e-clouds (WARP, C-MAD, HEADTAIL) have been very useful to analyze the bunch dynamics and derive reduced models as well as to generate analysis tools to process the measured data [5], [6], [7]. The ongoing effort is directed to include realistic feedback system models in the simulation codes to analyze the impact on the beam emittance and stability. A realistic simulation model for the feedback system must include the real number of samples per bunch processed by the feedback channel, modeling of technical limitations on the hardware components as well as feedback bandwidth and noise.

## MULTI-PARTICLE SIMULATION CODES

Simulation codes as HEADTAIL, C-MAD, WARP are used to analyze and estimate the behavior of the bunch interacting with electron clouds and machine impedances. The simulation code models the turn-by-turn interaction of a single bunch with an electron cloud and the machine impedance. In the case of electron clouds, the simulation takes into account the electron cloud produced by the preceding bunches, with a cloud density as inferred from previous simulations. Both protons and electrons are represented by macro-particles. The bunch is divided into  $N_{sl}$  longitudinal slices and interacts with the cloud on successive time steps. The transverse electrical interaction between the protons and the electrons of each slice and vice-versa is computed by a 2D particle-in-cell algorithm. The equations of motion for protons and electrons are: [7] [8]:

$$\begin{aligned} \frac{d^2 \vec{x}_{p,i}(s)}{ds^2} + \mathbb{K}(s) \vec{x}_{p,i}(s) &= \Delta \vec{P}_{e,i}(\vec{x}_{p,i}(s)) \quad (1) \\ \frac{d^2 \vec{x}_{e,j}(s)}{ds^2} &= \Delta \vec{P}_{p,j}(\vec{x}_{e,j}(s)) \end{aligned}$$

where the positions of electrons and bunch particles are represented by the vectors  $\vec{x}_e \equiv (x_e, y_e)$  and  $\vec{x}_p(s) \equiv (x_p, y_p)$  in (x,y,s) coordinates.  $\Delta \vec{P}_{e,i}(\vec{x}_{p,i}(s))$ ,  $\Delta \vec{P}_{p,j}(\vec{x}_{e,j}(s))$  are the scaled momenta applied to the protons and electrons, respectively, due to the proton-electron interaction.  $\mathbb{K}(s)$  is the transfer matrix between two subsequent interaction points.  $f_e(x, y, t)$  and  $f_{p,SL}(x, y)$  are the distribution functions of the electron cloud and of the bunch particles contained in one slice, respectively, which produce the electric field  $E_{e(p)}$ . Synchrotron motion is included in the simulations.

\* Work supported by the US-DOE under Contract DE-AC02-76SF00515 and US-DOE LARP program and DE-AC02-05CH11231

<sup>†</sup> rivetta@slac.stanford.edu

The feedback control system interacts with the multi-particle simulator by measuring the absolute transverse and longitudinal position of each slice centroid and generating a momentum or kick signal that drives each bunch slice. In (1), the momentum signal is modeled as an additive term in the proton differential equation,  $\Delta P_{T,x,y}(t)|_{SL}$ , for the  $SL^{th}$  slice. Similarly for the same slice, the measured centroids are defined by  $\langle x(t) \rangle_{SL} = \langle x f_p(x, y, s, t) \rangle_{SL} / \langle f_p(x, y, s, t) \rangle_{SL}$ . Similar definitions are used for  $\langle y(t) \rangle_{SL}, \langle s(t) \rangle_{SL}$  centroids. Fig.1 depicts a block diagram of the feedback control system for the vertical axis interacting with the proton bunch. In this plot, the vertical displacement of the centroid of 64 slices is labeled as  $\langle y(t) \rangle = [y_1(t), y_2(t), \dots, y_{64}(t)]^T$  and the momentum signal for those slices is  $\Delta P_{T,y}(t) = V_b(t) = [V_{b1}(t), \dots, V_{b64}(t)]^T$ . The feedback channel is defined by three major blocks: the receiver that measures and processes the signal from the beam pick-up and estimates the vertical position of the different areas of the bunch, the processing channel that computes, from the vertical signal, the appropriate control signal  $V_C(t)$  and the power stage (Amplifier, Kicker) that amplifies and delivers the momentum to different bunch slices.

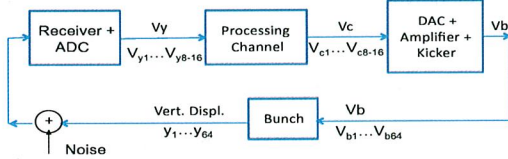


Figure 1: Block diagram of feedback control channel interacting with the proton bunch.

The implementation of these blocks introduces limitations in the level and frequency of the signals processed. Appropriate models of those blocks are necessary in the design and simulation of the feedback channel to understand the real limitations of the feedback channel in the stabilization of the bunch dynamics.

## FORMALISM FOR SIMULATION MODELS

The main idea is to characterize the response of each block in the feedback system on a fast-time scale and reduce the system dynamics by defining a map between a set of input samples  $y_{IN}$  and output samples  $y_{OUT}$ , where  $y_{OUT}, y_{IN}$  are vectors in  $\mathbb{R}$  at a particular time. In general, the vectors length is not the same.

The relationship between output-input signals for linear-time invariant (LTI) continuous systems is given by the convolution integral

$$y_{OUT}(t) = h(t) * y_{IN}(t) = \int_{-\infty}^{\infty} h(t - \tau) y_{IN}(\tau) d\tau, \quad (2)$$

where  $h(t) = \mathcal{L}^{-1}\{H(s)\}$  is the impulse response of the system,  $H(s)$  is the transfer function of the system in

Laplace domain and  $\mathcal{L}^{-1}\{\cdot\}$  is the inverse Laplace transform operator. Similarly for discrete systems and sampled signals the  $k^{th}$  sample of the output signal is

$$y_{OUT}(k) = \sum_{i=-\infty}^{\infty} h(k-i) y_{IN}(i) \quad (3)$$

with  $h(k)$  is the unit impulse response,  $h(k) = \mathcal{Z}^{-1}\{H(z)\}$ ,  $H(z)$  is the transfer function of the system in  $Z$  domain and  $\mathcal{Z}^{-1}\{\cdot\}$  is the inverse  $\mathcal{Z}$  transform operator. The transfer function for LTI system can be in general defined by an ARMA model or ratio between two polynomials

$$H(z) = \frac{A_1 z^{-1} + A_2 z^{-2} + \dots + A_m z^{-m}}{B_1 z^{-1} + B_2 z^{-2} + \dots + B_n z^{-n}} \quad (4)$$

if  $Y_{OUT}(z) = \mathcal{Z}\{y_{OUT}(k)\}$  and  $Y_{IN}(z) = \mathcal{Z}\{y_{IN}(k)\}$  are the  $Z$  transform of the output/input sampled signals, then

$$\frac{Y_{OUT}(z)}{Y_{IN}(z)} = H(z) = \frac{A_1 z^{-1} + A_2 z^{-2} + \dots + A_m z^{-m}}{B_1 z^{-1} + B_2 z^{-2} + \dots + B_n z^{-n}}, \quad (5)$$

then  $Y_{OUT}(z)(B_1 z^{-1} + B_2 z^{-2} + \dots + B_n z^{-n}) = Y_{IN}(z)(A_1 z^{-1} + A_2 z^{-2} + \dots + A_m z^{-m})$ . Applying the inverse  $\mathcal{Z}$  transform, it is possible to get the recursive relationship between input/output samples:  $B_1 y_{OUT}(k) + B_2 y_{OUT}(k-1) + \dots + B_n y_{OUT}(k-n-1) = A_1 y_{IN}(k) + A_2 y_{IN}(k-1) + \dots + A_m y_{IN}(k-m-1)$ . Assuming there are no samples from previous bunches interfering with the actual processed bunch,  $y_{IN}(k) = y_{OUT}(k) = 0, \forall k \leq 0$  and the maximum length of the signals is  $k = N_{sl}$ , the following sequences can be defined:

$$\begin{bmatrix} B_1 & B_2 & \dots & B_n & 0 & \dots & 0 \\ 0 & B_1 & B_2 & \dots & B_n & \dots & 0 \\ \dots & \dots & \dots & \dots & \dots & \dots & \dots \\ 0 & \dots & \dots & 0 & B_1 & B_2 & \dots \\ 0 & \dots & \dots & \dots & 0 & B_1 & \dots \end{bmatrix} \begin{bmatrix} y_{OUT}(N_{sl}) \\ y_{OUT}(N_{sl}-1) \\ \dots \\ y_{OUT}(2) \\ y_{OUT}(1) \end{bmatrix} = \begin{bmatrix} A_1 & A_2 & \dots & A_m & 0 & \dots & 0 \\ 0 & A_1 & A_2 & \dots & A_m & \dots & 0 \\ \dots & \dots & \dots & \dots & \dots & \dots & \dots \\ 0 & \dots & \dots & 0 & A_1 & A_2 & \dots \\ 0 & \dots & \dots & \dots & 0 & A_1 & \dots \end{bmatrix} \begin{bmatrix} y_{IN}(N_{sl}) \\ y_{IN}(N_{sl}-1) \\ \dots \\ y_{IN}(2) \\ y_{IN}(1) \end{bmatrix}$$

$$\begin{aligned} B y_{OUT} &= A y_{IN} \\ y_{OUT} &= B^{-1} A y_{IN} = M y_{IN} \end{aligned} \quad (6)$$

On the slow time scale, the matrix  $M$  operates as a gain between the  $y_{OUT}, y_{IN}$  variables. The matrix  $M$  does not necessarily have to be a square matrix. For a general block in the feedback channel, the matrix  $M$  can be calculated as the product of elemental matrices representing the ratio between internal variables in the block,  $M = M_1 M_2 \dots M_w$  for a block subdivided in  $w$  elemental stages.

## APPLICATION TO THE SPS RING

We present an application of this formalism with a simple case representing the SPS dedicated hardware to test the LARP wideband feedback system. This example is analyzed using the C-MAD code and by setting  $N_{sl} = 64$  and

$N_{control} = 16$  samples per bunch to process the feedback algorithm. This is equivalent to a 2.6 G Samples/sec sampling frequency in the ADC/ DAC and processing channel. This example describes some stages in the power block and the receiver block. The kicker structure installed in the SPS and dedicated for our studies is an 'exponential strip line' designed originally as a wide-band pick-up [9]. The kicker's frequency response was estimated by measuring the response of the structure as a pick-up. Fig. 2 depicts the estimated transfer function. This function is approximated by a transfer function  $H_k(\omega) = H_k(s)|_{s=j\omega}$ . Based on  $H_k(s)$  and applying  $\mathcal{Z}$  transform,  $H_k(z) = \mathcal{Z}\{H_k(s)\}$  is calculated as the ratio of two polynomials in  $z$  (Eqns. (4), (5)). After building the A and B matrices, (eqn. (6)), the matrix  $M_k$  representing the mapping between the kicker input voltage and the output momentum applied to each bunch slice is calculated. Similarly, the matrix  $M_{DAC}$  corresponding to the DAC response is calculated, while for the case of the wideband amplifier and cables, an ideal gain has been assumed given that the kicker's frequency response is dominant to characterize the power stage response.

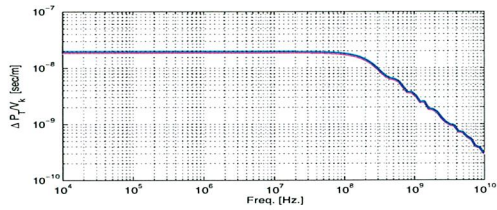


Figure 2: Frequency response of the kicker

We apply a kick to the bunch at turn number 20. Fig. 3 depicts the DAC input samples  $[V_{c1} \dots V_{c16}]$ . It compares the momentum applied to the bunch using time-domain analysis following eqn. (2) and using the matrix  $M_{PWR} = M_k M_{pwr} M_{DAC}$  in C-MAD.

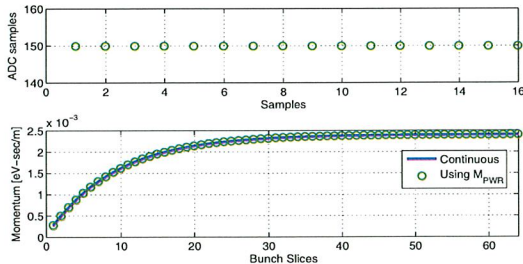


Figure 3: Power stage response

For the receiver, we assume that the signal  $\langle y(t) \rangle = [y_1(t) \dots y_{64}(t)]^T$  for  $t = kT_{rev}, k = 0, 1, \dots$  is the estimated vertical displacement for slices 1 to 64. Additionally, we assume that before the ADC, this signal is subject to an anti-aliasing filter with a bandwidth of 1.5 GHz. Fig. 4 shows the estimated vertical displacement of the bunch  $\langle y(t) \rangle$  after the kick was applied as measured at turn 29. This plot also show the filter output signal calculated using time domain analysis (eqn. (2)) and using the matrix  $M_f$ . The samples (ADC output) used in the processing channel  $[V_{y1} \dots V_{y16}]^T$  are calculated as  $V_y = M_{ADC} M_f \langle y \rangle$  in C-MAD.

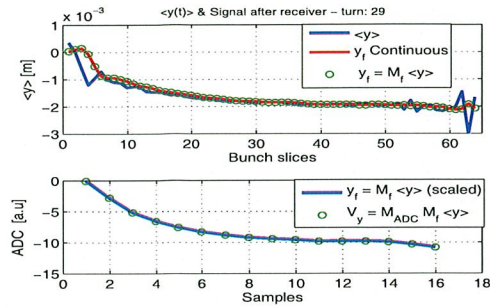


Figure 4: Receiver response

## CONCLUSIONS

We presented a formalism to model the response of different blocks of the feedback channels to include the limitations of real hardware units in multi-particle simulation codes. It allows to model Linear Time Invariant (LTI) systems and reduce the order of the system dynamics, considering the fast-time scale effects (nsec. time scale, bunch scale) in the slow time-scale (revolution period) as a matrix with constant coefficient coupling the different bunch samples. Results show that if the hardware stage is well represented by an LTI system model, the matrices obtained accurately describe its response in the slow-time scale.

## ACKNOWLEDGMENTS

We thank the SLAC AARD, CERN BE-RF departments, US LARP program for the support, and NERSC for the use of large scale computing facilities and technical support.

## REFERENCES

- [1] G. Arduini *et al.* 31<sup>st</sup> Advanced ICFA Beam Dynamics Workshop Napa, CA, USA, CERN-2005-001.
- [2] J.D. Fox *et al.*, "Feedback Techniques and Ecloud Instabilities - Design Estimates," PAC 2009, Vancouver, BC, Canada.
- [3] C. Rivetta *et al.*, "Feedback Control of SPS E-clouds / Transverse Mode coupling Instabilities," ELOUDS10 workshop, Cornell Univ., Ithaca, NY, USA.
- [4] J.D. Fox *et al.*, "SPS Eclouds Instabilities - Analysis of Machine Studies and Implications for Eclouds Feedback," IPAC 2010, Kyoto, Japan, pp. WEPEB052.
- [5] Jean-Luc Vay *et al.*, "Update on Electron-Cloud Simulations Using the Package WARP-POSINST," PAC 2009, Vancouver, BC, Canada, pp. FR5RFP077.
- [6] Mauro T. F. Pivi *et al.*, "C-MAD: A new self-consistent parallel code to simulate the electron clouds build-up and instabilities," Proc. of PAC 2007, Albuquerque, NM, USA.
- [7] G. Romulo *et al.*, "Practical user guide for HEADTAIL," CERN-SL-Note-2002-036.
- [8] Elena Benedetto, "Emittance growth induced by electron cloud in proton storage rings," Doctoral Thesis, POLITECNICO DI TORINO, Italy. CERN-thesis-2008-096.
- [9] R. Di Maria *et al.*, "Performance of Exponential Coupler in the SPS with LHC Type Beam for Transverse Broad-band Instability Analysis," 2009 DIPAC MOPD17.

This document was prepared as an account of work sponsored by the United States Government. While this document is believed to contain correct information, neither the United States Government nor any agency thereof, nor The Regents of the University of California, nor any of their employees, makes any warranty, express or implied, or assumes any legal responsibility for the accuracy, completeness, or usefulness of any information, apparatus, product, or process disclosed, or represents that its use would not infringe privately owned rights. Reference herein to any specific commercial product, process, or service by its trade name, trademark, manufacturer, or otherwise, does not necessarily constitute or imply its endorsement, recommendation, or favoring by the United States Government or any agency thereof, or The Regents of the University of California. The views and opinions of authors expressed herein do not necessarily state or reflect those of the United States Government or any agency thereof or The Regents of the University of California.